Tree Physiology, 2024, **44**, 246–259
https://doi.org/10.1093/treephys/tpae016
Advance access publication date 28 January 2024
Research paper

Temporal dynamics of stomatal regulation and carbon- and water-related traits for a native tree species in low subtropical China

Li-Wei Zhu[1,2], Yan-Qiong Li[1,2], Long-Wei Lu[1,2], Jing-Yi Wang[1,2], Jie Du[1,2] and Ping Zhao[1,2,*]

[1]South China Botanical Garden, Chinese Academy of Sciences, Xingke Road 723, Tianhe District, Guangzhou, 510650, China
[2]South China National Botanical Garden, Tianyuan Road 1190, Tianhe District, Guangzhou, 510650, China

*Corresponding author (zhaoping@scib.ac.cn)

Handling Editor: Henry Adams

Stomata are pivotal in modulating water and carbon processes within plants. However, our understanding of the temporal dynamics of water- and carbon-related traits, as influenced by stomatal behavior, remains limited. Here, we explore how stomatal regulation behavior and water- and carbon-related traits vary with changing environments by examining the seasonal variations in these traits of the native tree species *Schima superba* Gardn. et Champ. in low subtropical China. In February, April and July of 2022, a series of water- and carbon-related traits were measured in the leaves and stems. The results showed that *S. superba* exhibited isohydric behavior in February when the soil dried out and vapor pressure deficit (*VPD*) was lower but anisohydric behavior in April and July when the soil was wetter and *VPD* was higher. In February, nonstructural carbohydrates (*NSC*) and their components increased, and a relatively large contribution of soluble sugars to the change in *NSC* was observed. In the branches and phloem, *NSC* and their components displayed a relatively high monthly variability, suggesting their role in maintaining carbon balance within the trees. Conversely, the *NSC* in the leaves demonstrated minimal monthly variability. The specific leaf area, as well as the concentration of nitrogen (*N*) and phosphorus (*P*) per unit mass in leaves and the cumulative stem water release, exhibited a decrease with a reduction in soil water potential. Interestingly, the hydraulic conductivity remained consistent throughout this process. Furthermore, the relatively low monthly growth rate observed in February could suggest a carbon sink limitation. In conclusion, the increased *NSC* and decreased water status of *S. superba* under relatively stressed soil conditions indicated a trade-off between water and carbon storage. Our findings enhance our comprehension of the dynamics and regulation of water and carbon status in forests, thereby advancing the development of plant carbon and water process models under climate change scenarios.

Keywords: low subtropical China, nonstructural carbohydrate, sap flux, stomatal regulation, temporal dynamics.

Introduction

Over the past two decades, increasing drought and temperature stress due to intense anthropogenic activity have triggered widespread tree mortality and severe forest decline (Anderegg et al. 2013, Hartmann et al. 2018). Hydraulic failure, characterized by the blockage of water transport due to xylem embolism, and carbon starvation, marked by an inability to sustain metabolism due to a negative carbohydrate balance, are two of the main mechanisms driving mortality in forest trees under water stress (McDowell et al. 2008, Adams et al. 2009, Brodribb and Cochard 2009, Choat et al. 2012, Plaut et al. 2012). This underscores the pivotal role of carbon and water processes in modulating vegetation responses to environmental shifts.

Plant water-use strategies can be categorized along a continuum from isohydric to anisohydric based on stomatal behaviors in response to natural fluctuations in soil water status and evaporative demand (Tardieu and Simonneau 1998, McDowell et al. 2008, Klein 2014, Hochberg et al. 2018). Isohydric plants are capable of reducing stomatal conductance to sustain a constant midday leaf water potential when confronted with carbohydrate depletion under decreasing soil water potential and air-drying conditions, whereas anisohydric species allow water potential to decrease and maintain carbon assimilation rates at the expense of hydraulic failure (McDowell et al. 2008). To date, numerous studies have reported the responses of isohydric and anisohydric species to drought (Garcia-Forner et al. 2017, Yi et al. 2017, Fu et al. 2019). However, Hochberg et al. (2018) presented the opinion that iso/anisohydric behavior varied with soil water potential. The ecosystem- and species-level analyses based on the published field observations by Wu et al. (2021) confirmed the aforementioned conclusion. The Sangiovese grape variety exhibited anisohydric behavior at a soil water potential greater than −0.6 MPa, but adopted an isohydric strategy when the soil water potential ranged between −0.6 MPa and −1.1 MPa (Poni et al. 2007). In accordance with a minimal model that is grounded in Darcy's law, it has been observed that plants exhibit anisohydric characteristic under conditions of abundant water availability, specifically when the soil water potential exceeds −0.5 MPa (Hochberg et al. 2018). Similar findings have been reported in other studies that indicate an increase isohydry in soil water stress and an increase anisohydry in high soil water availability (Collins et al. 2010, Domec and Johnson 2012, Zhang et al. 2012, Meinzer et al. 2016). In other words, the classification of iso/anisohydry may show a temporal trend with changing environmental conditions. However, few studies have examined the temporal

Received: August 9, 2023. **Revised:** December 22, 2024. **Accepted:** January 21, 2024

patterns of stomatal regulation behavior. Consequently, it is imperative to conduct studies on the same species across a spectrum of environmental conditions in order to differentiate between iso- and anisohydric behaviors (Hochberg et al. 2018).

In most studies, iso/anisohydry has been defined by alterations in midday leaf water potential in responses to shifts in soil water potential during prolonged drought conditions (Meinzer et al. 2016, Martínez-Vilalta and Garcia-Forner 2017, Hochberg et al. 2018). However, the initial article, which described iso/anisohydric behavior, emphasized that isohydric species not only depend on soil water status, but also maintain a stable leaf water potential in response to evaporative demand during the day (Tardieu and Simonneau 1998). Anisohydric species demonstrate accelerated stomatal responses and a decrease in leaf water potential as evaporative demand increases during the day (Tardieu and Simonneau 1998, Meinzer et al. 2017). In contrast, Fu et al. (2019) indicated that stomatal responses to evaporative demand were not related to the iso/anisohydric strategy. Because Meinzer et al. (2017) and Fu et al. (2019) conducted irrigated experiments in the same climate-controlled greenhouse, the stomatal response of natural forests to evaporative demand during the day may appear inconsistent with their results. Thus, in addition to the change in water potential with soil water status, stomatal responses to evaporative demand could also be used to assess iso/anisohydry in the field.

The increase in nonstructural carbohydrates (*NSC*) due to elevated atmospheric CO_2 levels has the potential to alleviate tree mortality caused by drought (Liu et al. 2017, Li et al. 2018, 2022). This highlights the significance of carbon storage capacity within plants in response to climate change. Regardless of phenology, plants with higher *NSC* exhibited enhanced drought resistance due to osmoregulation, defense mechanisms and embolism repair (Woodruff and Meinzer 2011, Woodruff et al. 2015, Tomasella et al. 2019, Trifilò et al. 2019). In addition to alterations in plant water status, *NSC* may also be influenced by changes in source–sink activity due to stomatal regulation behavior (Dietze et al. 2014, Signori-Müller et al. 2021). For instance, *Populus bolleana* Lauche, characterized by its tight stomatal control, exhibited *NSC* depletion in its branches during extended drought periods compared with *Haloxylon ammodendron*, which possesses weaker stomatal control (Xu et al. 2023). However, Jiang et al. (2021) showed that species with more isohydric strategies accumulated *NSC* in the dry season due to high photosynthetic rates and hydraulic capacitance. In contrast, Körner (2003) and Würth et al. (2005) indicated that the increase in *NSC* during dry seasons due to starch was caused by restricted growth rather than photosynthesis. In addition to the influence of photosynthesis and growth status on *NSC*, carbohydrate reserves were unable to be utilized during a phloem transport failure due to the presence of positive hydrostatic pressure in the xylem caused by high xylem tension during drought conditions (Hölttä et al. 2009, Ruehr et al. 2009, McDowell and Sevanto 2010, Adams et al. 2013). However, water stored in plants can serve as a buffer against xylem stresses (Scholz et al. 2011, Kocher et al. 2013, Kaplick et al. 2018, Janssen et al. 2020), thereby facilitating the preservation of hydraulic integrity and physiological activity. In comparison with anisohydric species, isohydric species exhibited a stronger reliance on stored water rather than *NSC* depletion during dry seasons (Kumagai et al. 2009, Kocher et al. 2013, Matheny et al. 2015, Jiang et al. 2021). Conversely, the use of water storage to sustain elevated transpiration rates and the accumulation of *NSC* during drought in anisohydric species has been reported in previous studies (Yi et al. 2017, Xu et al. 2023). Therefore, the discrepancy between studies underscores the need to elucidate the relationship between water and carbon processes in plants and stomatal control to understand forest dynamics under changing environments.

In this study, we hypothesized that (i) tree species show isohydric behavior at low soil water potential and anisohydric behavior at a sufficient soil water status, and (ii) seasonal changes in stomatal regulation behavior are associated with the water status of xylem and *NSC*. To test the aforementioned hypotheses, we measured sap flux density and stem radius changes at breast height, leaf water potential, *NSC* concentrations in four tissues (namely, leaves, branches, xylem and phloem), and other water- and carbon-related traits of leaves and stems across seasons for a native tree species, *Schima superba* Gardn. et Champ., in low subtropical China.

Materials and methods

Site description

This study was conducted at the *S. superba* plantation (23°10′ N, 113°21′ E and 41 m elevation) located in the South China National Botanical Garden in Guangzhou, Guangdong Province, China. This region is characterized by an Asian monsoon climate, which is distinguished by its mild winters and hot, rainy and humid summers. The average annual temperature and precipitation in the region are 20.9 °C and 2079.6 mm, respectively, as per data from 2012 to 2021 (Ouyang et al. 2022). Notably, 78.7% of the average annual precipitation occurs between April and September, constituting the wet season in this area (Figure S1a available as Supplementary data at *Tree Physiology* Online). During the dry season, which spans from October to March, there is a significant decrease in the ratio of precipitation to evapotranspiration (an indicator of the drought index) compared with the wet season (Figure S1b available as Supplementary data at *Tree Physiology* Online; 0.61 vs 1.38; $P < 0.05$; $n = 10$). The division of dry and wet seasons mentioned above was consistent with that in some previous studies in low subtropical China, such as the study by Zhu et al. (2013). The soil is identified as a loam type, exhibiting a pH of 4.10, organic matter content of 22.52 g kg^{-1}, total nitrogen content of 0.68 g kg^{-1} and available phosphorus contents of 1.74 mg kg^{-1}. *S. superba* dominates the evergreen broad-leaved forests, characteristic of subtropical regions. This light-demanding species undergoes a phase of new leaf production in February, followed by rapid growth from early July to early September, and lignification between mid-September and the end of October. This plantation was established in the mid-1980s. The plant density is 767 trees ha^{-1}, as determined by a survey conducted on a 30 m × 20 m plot in 2023. Recently, the understory has been predominantly inhabited by *Psychotria rubra* (Lour.) Poir. var. rubra.

Environmental variables

Photosynthetically active radiation (*PAR*), air temperature (*T*) and relative humidity (*RH*) were monitored using SQ (Apogee Instruments, USA) and HygroVUE5 sensors (Campbell Scientific, USA) mounted on a tower above the canopy in the

Table 1. Tree height (H, m), diameter at breast height (DBH, cm) and crown area (C_a, m^2) of five sample trees.

No.	H	DBH	C_a	F_d monitoring
1	16.53	29.50	30.60	•
2	18.13	28.05	17.02	•
3	16.97	28.80	22.79	•
4	14.83	15.50	5.70	
5	16.83	36.40	20.68	•
Mean	16.66 (0.53)	27.65 (3.38)	19.36 (4.07)	

Standard errors are shown in parentheses. • indicates sample trees with sap flux probes.

plantation. The vapor pressure deficit (VPD) was determined using the equation provided below (Campbell and Norman 1998):

$$VPD = \mathbf{a} \times \exp\ [\mathbf{b} \times T/(\mathbf{c} + T)] \times (\mathbf{1} - RH) \quad (1)$$

where a, b and c are constants.

Tree properties

Diameter at breast height (1.3 m above ground, DBH), crown width in two perpendicular directions and tree height (H) were measured using a diameter tape, measuring tape and VERTEX IV dendrometer (Haglöf Inc., Sweden), respectively. The area of the crown (C_a, m^2) was calculated by multiplying the widths of the crowns in both vertical directions. The properties of the trees are listed in Table 1. To collect the leaves and branches of the tree crown, five trees were selected in close proximity to the observation tower. The size of the sample tree is distributed on both sides of the DBH frequency distribution (Figure S2 available as Supplementary data at *Tree Physiology* Online). Because the coordinated relationships between water- and carbon-related traits were revealed by analyzing their seasonal patterns at the whole-plant level, we did not consider the influence of tree size on the reliability of the results. The stand-level leaf area index (LAI) was determined through the utilization of the LAI-2200c plant canopy analyzer (LI-COR, Inc., USA) by randomly selecting multiple points on a monthly basis. The leaf area (A_L) and sapwood area at breast height (A_s) of individual sample trees were calculated based on the allometric relationship between A_L or A_s and DBH, as established for other individual trees near the experimental site as follows:

$$\log\ (A_L) = 1.6722 \times \log\ (DBH) + 3.1988\ \ (n = 5) \quad (2)$$

$$A_s = 0.6841 \times (DBH)^{2.0266}\ \ (n = 15) \quad (3)$$

Moreover, accounting for the seasonal variations in leaf area, the leaf area of each sample tree (A_L') was adjusted by the seasonal changes in LAI.

Leaf water potential

Three to five branches with leaves of sample trees exposed to the sun were cut for leaf water potential (ψ_L, MPa) measurements using a pressure chamber (1000; PMS Instrument Co., USA) every hour from 5:00 h in the wet season and 6:00 h in the dry season to 19:00 h (Beijing Standard Time) on the sunny days of 15 February, 7 April and 10 July 2022. The predawn ψ_L ($\psi_{L\text{-pre}}$) and midday ψ_L ($\psi_{L\text{-mid}}$) were taken as the ψ_L measured at either 5:00 h or 6:00 h and the lowest ψ_L during the day, respectively. Due to the disequilibrium between $\psi_{L\text{-pre}}$ and soil water potential (Bucci et al. 2005, Novick et al. 2022), three branches of each of the three sample trees were wrapped in aluminum foil and cling wrap after sunset on the day before the experiment and then measured simultaneously with $\psi_{L\text{-pre}}$ to represent soil water potential.

Sap flux density, canopy-level transpiration and mean stomatal conductance

Two 2-cm-long probes were installed on the north side of the four sample trees, ~15 cm apart to monitor sap flux density (Granier 1987). The probes were covered with a plastic box and an aluminum shield to protect them from rain and direct sunlight. The sap flux density per unit sapwood area (F_d, g m^{-2} s^{-1}) was determined using an empirical relationship based on the temperature difference between two probes and measured at 30-s intervals, averaged every 10 min, and recorded with a data logger (DL2e; Delta-T Devices, Ltd, Cambridge, UK). When scaling F_d to canopy-level transpiration, it is crucial to consider the radial and circumferential variations in F_d, as well as tree length (time lag) and stem water storage. The nonsignificant difference in F_d among the different stem directions of *S. superba* (Zhang et al. 2016) suggested that F_d on the north side of the trees could represent the average sap flux in this study. A small effect of stem water storage on transpiration at the canopy level was demonstrated from a widely published data set (Oren et al. 1999). Furthermore, even in northern China, where there is a relatively large water deficit, only 6% to 7% of the sap flux is stored in the stems of coniferous and broad-leaved tree species (Liu et al. 2021). We hypothesize that the contribution of water storage to canopy-level transpiration may have been overlooked in southern China, where rainfall is abundant. According to the diurnal pattern of F_d and PAR, sap flux at breast height started ~20 min after the initiation of PAR (Figure S3 available as Supplementary data at *Tree Physiology* Online). Thus, this time lag was implicated in scaling F_d to canopy-level physiological parameters.

At this study site, the radial F_d patterns showed no significant difference in F_d at the 0–2 and 2–4 cm depths, whereas F_d was 15% lower at a depth of 4–6 cm than that in the outermost 4 cm (Zhang et al. 2016). The sapwood depths (D_s) of the sample trees monitored in our study were 3.76, 3.57, 3.66 and 4.66 cm. Thus, the F_d of the sample trees with $D_s <$ 4 cm represented the mean sap flux density of all the sapwood, and the mean F_d (F_d') of the fourth sample tree with $D_s > 4$ cm was calculated as follows:

$$F_d' = \left[F_d \times A_{s(0-4)} + 0.85 \times F_d \times A_{s(D_s-4)}\right]/D_s \quad (4)$$

where $A_{s(0–4)}$ is the A_s in the outermost 4 cm of sapwood and $A_{s(Ds-4)}$ is the A_s at a sapwood depth after subtracting the outermost 4 cm from the whole sapwood depth.

To evaluate the efficiency of water transport in the stem xylem, the daily stem hydraulic conductivity (K_s) was determined by calculating the slope of the linear relationship between the mean F_d' of the sample trees and ψ_L in each month.

The transpiration rate per unit leaf area (E_L, g m^{-2} s^{-1}) was calculated as follows:

$$E_L = F_d' \times A_s / A_L' \quad (5)$$

The *LAI* was 1.82 (±0.02), 2.77 (±0.04) and 2.94 (±0.12) m^2 m^{-2} in February, April and July of 2022, respectively, indicating a good coupling between the canopy and the surrounding atmosphere in this plantation. Therefore, the mean canopy stomatal conductance (G_s, mol m^{-2} s^{-1}) was calculated as follows (Schäfer et al. 2000):

$$G_s = (G_v \times T_k \times V_m \times E_L) / VPD \quad (6)$$

where G_v is the universal gas constant adjusted for water vapor, T_k is the air temperature in Kelvins (K) and V_m is the molar volume of the gas.

Characteristics of iso/anisohydry under changing soil water status and *VPD*

The behavior of stomatal regulation was evaluated based on the stomatal responses to *VPD* during the day and soil water potential across seasons. First, the correlation between daily G_s and *VPD* under unconstrained light conditions (approximately photosynthetically active radiation >1000 μmol m^{-2} s^{-1}) was determined as follows (Oren et al. 1999):

$$G_s = G_{sref} - m \times \ln(VPD) \quad (7)$$

where G_{sref} is the reference G_s value at a *VPD* of 1 kPa and m, as $dG_s/dln(VPD)$, is the stomatal sensitivity to *VPD*. The shallow slope of the relationship between $dG_s/dln(VPD)$ and G_{sref}, $dG_s/dln(VPD)/G_{sref}$, suggests a less strict regulation of leaf water potential with increasing *VPD* (Oren et al. 1999).

Second, using the definition framework of Roman et al. (2015) and Yi et al. (2017), the correlation between the water potential gradient ($\Delta\Psi$) and G_s across seasons can be determined as follows:

$$G_s = \frac{1}{VPD} \times K_s \times (\Delta\Psi) \quad (8)$$

where K_s is the whole-plant hydraulic conductance and gravitational contribution to water potential is neglected, and $\Delta\Psi = \Psi_s - \Psi_L$, with Ψ_s representing the soil water potential. Assuming that K_s remains constant with soil water status, for isohydric behavior, $\Delta\Psi$ decreases as Ψ_L remains constant, and G_s and its sensitivity to *VPD* decrease during drought periods compared with the water-abundant period. As there was no difference in $\Psi_{L\text{-pre}}$ between April and July, this definition framework could not be used to characterize iso/anisohydry in these two months.

Leaf and stem traits

During the ψ_L measurement, ~10 leaves per sample tree were collected for leaf trait measurements. After the leaf area was measured using a LI-3000C leaf area meter (LI-COR, Inc., USA), the leaves were dried at 65 °C to constant weight, and then the dry weight was measured. The specific leaf area (*SLA*) was calculated by dividing leaf area by dry weight. Given that leaf traits exhibit a stronger and simpler coordination on a mass basis, and are closely associated with growth rates (Lambers and Poorter 1992, Wright et al. 2004), nitrogen (*N*) and phosphorus (*P*) concentrations were expressed on a mass basis. Leaf N and P concentrations per unit mass (N_{mass} and P_{mass}, respectively) were determined using the oxidation–reduction method with a MACRO cube elemental analyzer (Elementar, Germany) and P-V-Mo colorimetry with an L6S ultraviolet spectrophotometer (INESA Scientific Instrument Co., Ltd, Shanghai, China), respectively.

During the experiment, the outermost sapwood at breast height was collected and immediately transferred to the laboratory. After measuring the fresh weight (W_f, g), the volume of wood (V_w, cm^3) was determined using a volumetric displacement method. The samples were immersed in ultrapure water until a constant weight was achieved. The saturated weight (W_s, g) was measured. The samples were then dried to constant weight at 65 °C, and the dry weight (W_d, g) was measured. The wood density (*WD*) was calculated as W_d/V_w. The relative water content (*RWC*) was expressed as the ratio of the stem segment's water to its maximum mass of stored water, calculated using the following formula:

$$RWC = (W_f - W_d) / (W_s - W_d) \quad (9)$$

The cumulative water release in the stem (*CWR*, g cm^{-3}) was employed to evaluate the xylem hydraulic capacitance, calculated using the following formula (Jiang et al. 2021):

$$CWR = (1 - RWC) \times (W_s - W_d) \times (1000 \times WD / W_d) \quad (10)$$

The daily stem circumference fluctuations (μm) were monitored using a DC3 series dendrometer (Ecomatik, Germany) on two sample trees (No. 3 and 4) in close proximity to the sap flux density monitoring positions and recorded synchronously with the sap flux. Increased stem shrinkage during the day is indicative of a greater depletion of stem water storage (Steppe et al. 2015). The daily range of stem circumference (C_r, μm) was used to assess water storage withdrawal and was calculated by subtracting the minimum stem circumference from the maximum per day. The monthly growth rate (*CG*, μm) was calculated as the difference between the maximum stem circumference measured on the first day and that measured at the end of the month. The daily shrinking and swelling of the stem (a process known as depletion and replenishment of stem water reserves) was determined using the stem size at 0:00 h of the day as a reference point. Namely, if the data measured with the dendrometer were above 0 μm, this indicated stem swelling and vice versa.

Nonstructural carbohydrates

Approximately 10 leaves, branches without leaves, outermost sapwood and phloem at breast height were collected and placed in a polystyrene box with ice on the same day that ψ_L

was measured. Because the bark may have negligible effects on branch *NSC* (Würth et al. 2005), the bark of branches was retained in this study. After measuring the fresh weight, samples were oven-dried at 105 °C for 30 min to inhibit enzymatic activity and then at 65 °C to a constant weight. Dried samples were ground to a fine powder and sieved through 100-mesh sieves. *NSC* are defined as a combination of soluble sugar and starch. The concentrations of soluble sugars (*SS*, %) and starch (%) were measured by the anthrone colorimetry method. A dry sample (0.5 g) was poured into a centrifuge tube (50 mL), 10 mL 80% ethanol was added and the mixture was stirred continuously in an 80 °C water bath for 30 min. After centrifugation, the supernatant was collected, the residue was repeatedly extracted twice with 10 mL 80% ethanol, and all supernatants were then combined and volumed with 80% ethanol. The *SS* extraction residue was transferred to a 50-mL volumetric flask, combined with 20 mL hot distilled water, boiled in a boiling water bath for 30 min, extracted with 9.2 mol L^{-1} perchloric acid for 15 min and then thoroughly mixed after cooling. After centrifugation at 4000 r.p.m. for 10 min, the residue was repeatedly extracted with 10 mL distilled water until the starch hydrolysis completeness test no longer showed blue. The supernatant was combined and diluted to 100 mL with distilled water. The starch and *SS* concentrations were determined using an ultraviolet spectrophotometer (UV-1800PC; Mapada Inc., Shanghai) and a standard curve. The ratio of *SS* to starch (*SS*/starch) was calculated to examine the variation in *SS* relative to starch, as the rate of change in *SS* and starch can differ in a changing environment.

Statistical analyses

The comparison of environmental factors across seasons was conducted using a one-way ANOVA. The $\psi_{L\text{-pre}}$ of both the covered and uncovered branches with aluminum foil were compared utilizing the *t*-test for paired samples. The comparison of $\psi_{L\text{-pre}}$ and $\psi_{L\text{-mid}}$ across seasons was conducted using a repeated-measures general linear model. The linear relationship's slope between mean F_d' and $\ln(-\psi_L)$, G_s and $\ln(VPD)$, and G_s and ψ_L, as well as the intercept of this relationship between mean F_d' and $\ln(-\psi_L)$ (reference F_d'), G_s and $\ln(VPD)$ (G_{sref}) for sample trees across different months, were compared using a univariate analysis of variance within the general linear model. The *NSC*, *SS* or starch concentrations, as well as the *SS*/starch in leaves, branches, sapwood and phloem at breast height across seasons and tissues were compared using a repeated-measures general linear model. The interactive effects of tissue and season on *NSC*, *SS* and starch were considered. When the interactive effects were significant, a simple main effect was performed using the 'EMMEANS' function. The seasonal variations in leaf and stem traits (*SLA*, N_{mass}, P_{mass} and *CWR*) were assessed using a repeated-measures general linear model. Pairwise comparisons were conducted using the Bonferroni or least significant difference adjustment. The above analyses were performed using SPSS software (version 16.0; IBM SPSS Statistics, USA). The relative importance of *SS* and starch for *NSC* variation across seasons was analyzed using the lmg approach of the relaimpo package developed by Grömping (2007) in R software (version 4.1.2, R Core Team 2021). The seasonal variability of *NSC* and their components was determined using the quartile coefficient of dispersion (*QCD*) (Rosas et al. 2019), which was calculated based on the lower and upper quartiles in Microsoft Excel version 16 (Zhu and Zhao 2023).

Results

There was a distinct difference in *VPD* across seasons (Figure 1). The diurnal maximum *VPD* in February (1.14 ± 0.11 kPa) was lower than that in the other two months. However, there was no significant difference in the diurnal maximum *VPD* in April and July (3.07 ± 0.31 and 3.29 ± 0.14 kPa in April and July, respectively). There was no significant difference in ψ_L between aluminum foil-wrapped leaves and unwrapped leaves (data not shown, $P > 0.05$), suggesting that $\psi_{L\text{-pre}}$ can be considered as an indicator of soil water potential. As shown in Table 2, the $\psi_{L\text{-pre}}$ was significantly lower in February than in April and July, indicating a relatively high level of soil water stress in February.

Variations in leaf water potential and mean canopy stomatal conductance across seasons

$\psi_{L\text{-mid}}$ in February was not significantly different from that in April and July, while it was lower in July than in April (Table 2), indicating that *S. superba* showed isohydric behavior at lower soil water potential. The diurnal patterns of G_s and ψ_L showed a single peak type (Figure 2a). Compared with February, ψ_L remained stable for a relatively long period at midday in April and July. Based on the pooled data from the four sample trees, G_s exhibited an increase with a decrease in ψ_L in February and April. However, no discernible correlation between G_s and ψ_L was observed in July (Figure 2b). Although the slope of the regression line correlating G_s with ψ_L was relatively steep in February compared with April, this difference lacked statistical significance.

In unconstrained light conditions, G_s decreased with *VPD* increased (Figure 3). G_{sref} exhibited significant seasonal variations (8.10 mmol m^{-2} s^{-1}, 17.14 mmol m^{-2} s^{-1} and 14.62 mmol m^{-2} s^{-1} in February, April and July, respectively), with the lowest value in February and the highest value in April ($P < 0.01$). The stomatal sensitivity to *VPD* ($dG_s/d\ln(VPD)$) was significantly higher in April than in February and July. Meanwhile, $dG_s/d\ln(VPD)/G_{sref}$ was relatively high in February compared with in April and July, at 0.81, 0.51 and 0.49, respectively, which was consistent with the narrow *VPD* range in February (0.91–1.83, 2.07–4.50 and 2.06–3.37 kPa in February, April and July, respectively), suggesting strict stomatal regulation of ψ_L in February and less strict stomatal regulation in April and July as *VPD* increased.

Variations in nonstructural carbohydrates, soluble sugars, starch concentration and the ratio of soluble sugar to starch across tissues and seasons

Interactive effects of tree tissue and season on variations in *NSC*, *SS* and starch concentrations were observed ($P < 0.01$). Pairwise analyses revealed that the *NSC*, *SS*, starch concentration and *SS*/starch were generally higher in February than in the other two months (Figure 4). In February, the *NSC* in phloem was higher than that in the other three tissues, and *SS* in leaves and phloem was higher, which led to a higher *SS*/starch in these two tissues than in the other tissues.

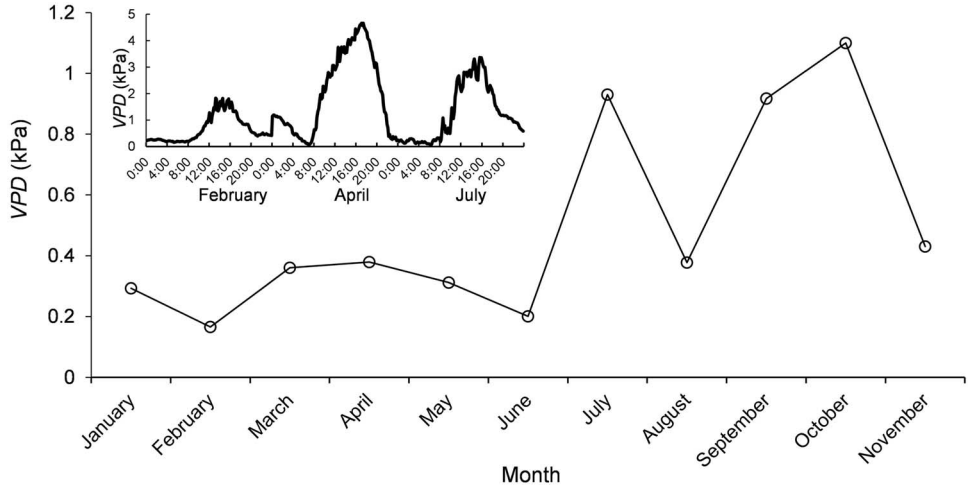

Figure 1. Monthly mean vapor pressure deficit (*VPD*) in 2022. Data for December are missing. The diurnal pattern of *VPD* during the experiment on 15 February, 7 April and 10 July 2022 is shown in the insert.

Table 2. Comparisons of predawn ($\psi_{L\text{-}pre}$, MPa) and midday ($\psi_{L\text{-}mid}$, MPa) leaf water potential across seasons (in February, April and July).

	February	April	July	*F*	*P*	Effect size
$\psi_{L\text{-}pre}$	−0.25 (0.02)b	−0.19 (0.02)a	−0.17 (0.01)a	16.62	0.001	0.68
$\psi_{L\text{-}mid}$	−1.22 (0.05)ab	−1.04 (0.02)a	−1.47 (0.11)b	9.19	0.008	0.52

Standard errors are shown in parentheses. Different letters indicate significant differences in ψ_L between months.

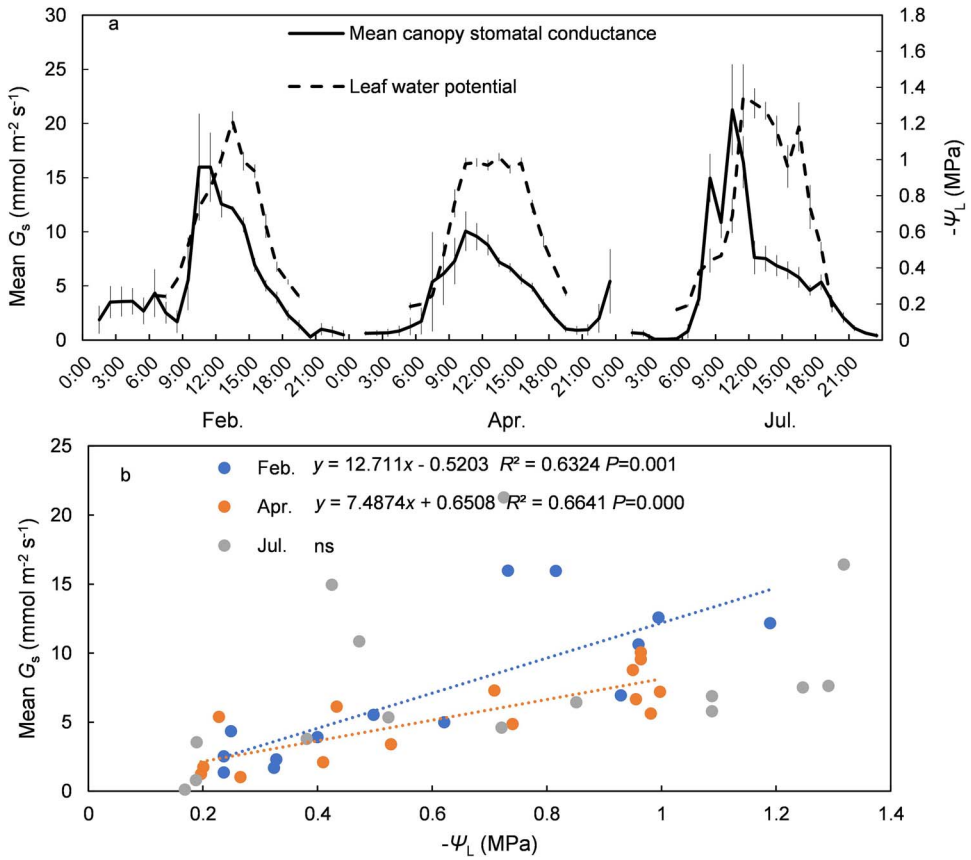

Figure 2. Diurnal patterns of mean canopy stomatal conductance (G_s) and leaf water potential (Ψ_L) (a) and their correlation (b) during the experiment on 15 February, 7 April and 10 July 2022. Each data point represents the mean G_s and Ψ_L of the sample trees. Panel (b) shows the linear regression model, and ns shows no significant correlation between the mean G_s and Ψ_L in July.

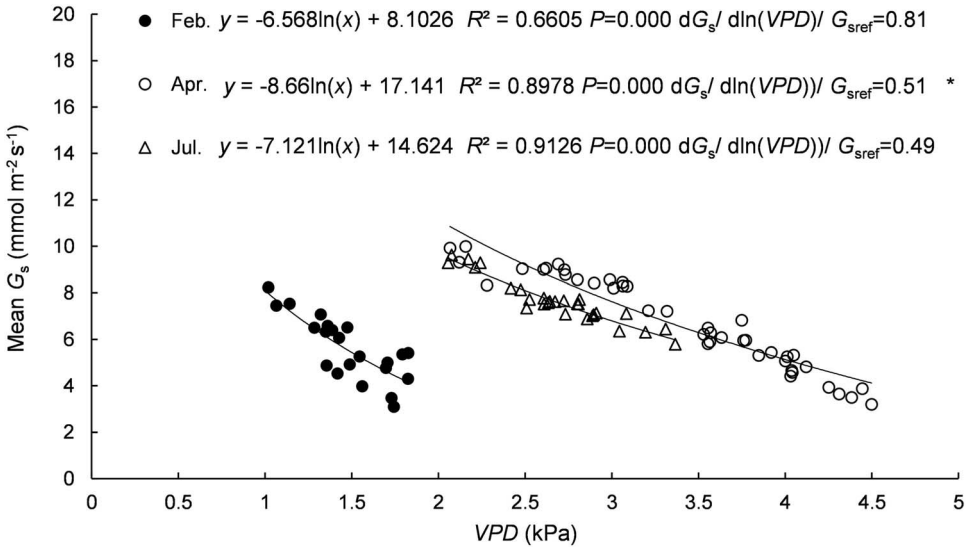

Figure 3. Relationship between mean canopy stomatal conductance (G_s) and vapor pressure deficit (*VPD*) on 15 February, 7 April and 10 July 2022. Data were selected under conditions where light may not have been limiting. G_{sref} is the reference G_s value at a *VPD* of 1 kPa. The asterisk represents a significant difference in stomatal sensitivity to *VPD* in April compared with the other two months at $P < 0.05$.

Table 3. Quartile coefficient of dispersion (*QCD*) of nonstructural carbohydrates (*NSC*), soluble sugar (*SS*), starch concentration and the ratio of *SS* to starch (*SS*/starch) in four tree tissues (leaf, branch, stem sapwood and stem phloem at breast height) across seasons.

	NSC	*SS*	Starch	*SS*/starch
Leaf	0.08	0.27	0.11	0.30
Branch	0.24	0.20	0.27	0.22
Sapwood	0.17	0.22	0.21	0.26
Phloem	0.24	0.33	0.21	0.27

The ratio of *SS* to starch concentration in the leaves was higher in February, while other tissues showed no change in *SS*/starch across seasons. As shown in Table 3, compared with the other three tissues, the high *QCD* of *SS* and the relatively low *QCD* of *NSC* and starch in leaves may have caused the relatively high *QCD* of *SS*/starch in leaves across seasons. In both branches and phloem, the *QCD* of *NSC* was relatively high across seasons, suggesting a high plasticity in response to fluctuating environmental conditions. The relative importance of *SS* and starch for changes in *NSC* was found to be 61.57% and 38.43%, respectively (Figure 5).

Variations in leaf and stem traits across seasons

Specific leaf area, P_{mass} and *CWR* were lower in February than in April and July, whereas N_{mass} was lower in February than in July and did not significantly differ in April compared with in February and July (Table 4). The *CG* of the two sample trees was relatively low in February compared with that in the other two months. The daily dynamics of stem circumference at breast height differed between the two tree samples (Figure 6). In No. 3, the stem water reserves exhibited a state of replenishment during the morning, with depletion beginning in the afternoon (approximately at 12:00 h or 14:00 h). This trend is likely attributable to diurnal variations in sap flux density. Specifically, for No. 3, the daily variation range of stem circumference was 64, 168 and 288 μm on 15 February, 7 April and 10 July 2022, respectively. Likewise, the depleted water storage was relatively low in February than in the other two months, as indicated by the small value of < 0 μm, which was consistent with a lower *CWR*. The mean F_d' increased logarithmically with decreasing ψ_L. The estimated stem hydraulic conductivity (K_s, slope of the relationship between mean F_d' and ψ_L) did not significantly differ among months, although it was relatively high in April compared with the other two months (Figure 7, data not shown, $F = 3.762$ and $P = 0.064$ for February vs. April, $F = 3.861$ and $P = 0.060$ for April vs. July, and $F = 0.003$ and $P = 0.958$ for February vs. July). The intercepts of the relationship between mean F_d' and ψ_L (a proxy for reference F_d') were found to be 22.514 g m^{-2} s^{-1}, 33.796 g m^{-2} s^{-1} and 29.897 g m^{-2} s^{-1} in February, April and July, respectively, with February having a smaller intercept (lower reference F_d') than April and July.

Discussion

This study elucidated the temporal dynamics of stomatal responses to soil water potential and *VPD*, stem hydraulic conductivity, stem radial growth and water status, *NSC*, *SLA*, N_{mass} and P_{mass} for *S. superba*, a native tree species in low subtropical regions of China. Smaller stomatal sensitivity to *VPD* ($dG_s/dln(VPD)$) and reference stomatal conductance (G_{sref}) and constant $\Psi_{L\text{-}mid}$ in relatively water-stressed months (February) compared with that during the period of relatively sufficient soil water (April and July), as shown in Table 2 and Figure 3, indicated an isohydric characteristic, whereas relatively low $dG_s/dln(VPD)/G_{sref}$ and variable $\Psi_{L\text{-}mid}$ in April and July illustrated an anisohydric behavior, supporting our first hypothesis. A higher *NSC*, their two components, and *SS*/starch in February than in the other two months and a relatively large contribution of *SS* to the seasonal variation in *NSC* relative to starch were found, suggesting the demand of *NSC* for osmoregulation under unfavorable soil water conditions. The reduced photosynthetic capacity (lower

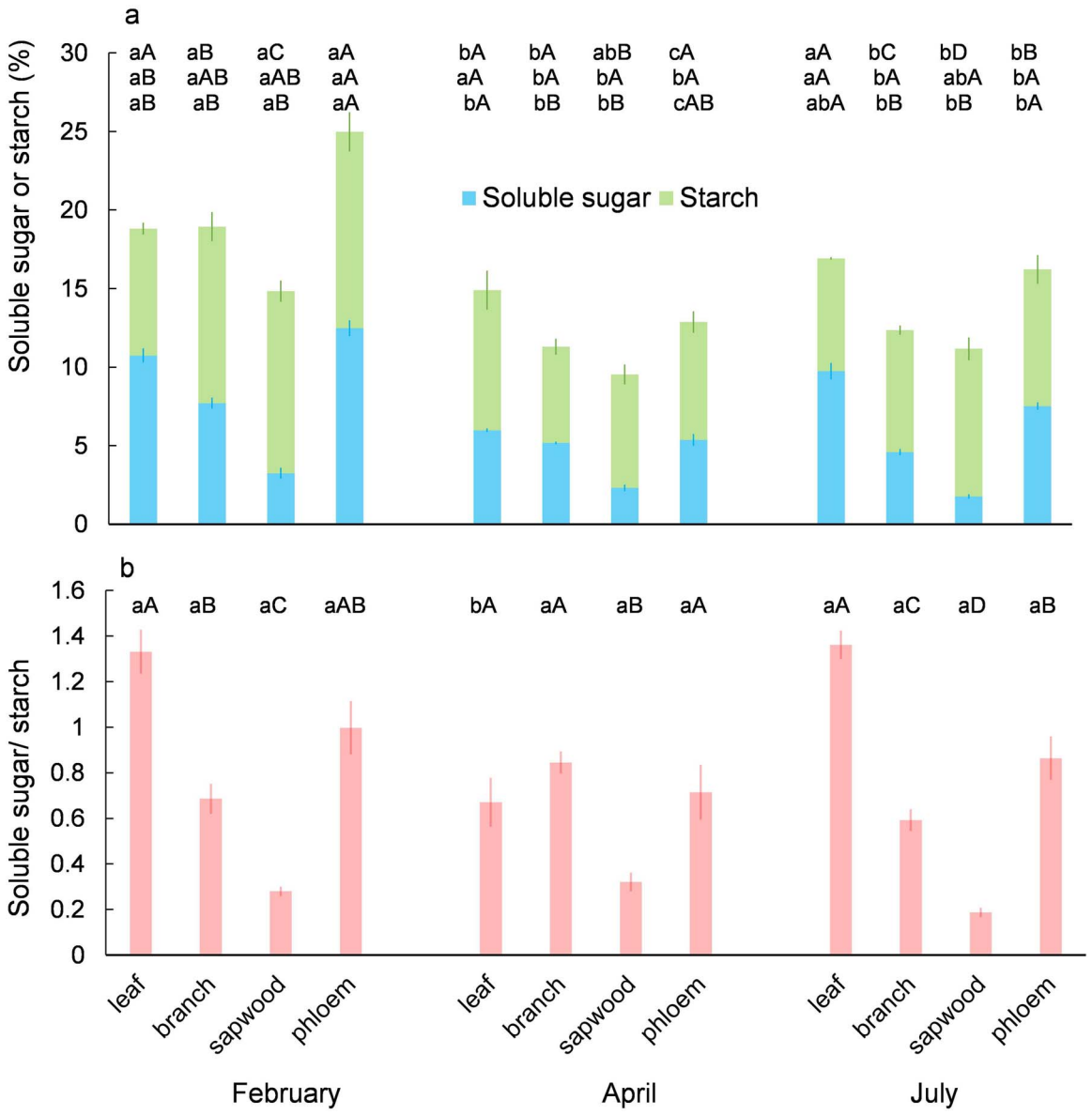

Figure 4. Concentrations of soluble sugar, starch and ratio of soluble sugar to starch (soluble sugar/starch) in four tree tissues (leaf, branch, stem sapwood and stem phloem at breast height) across seasons (in February, April and July). Different lowercase and uppercase letters represent significant differences in the concentrations of soluble sugar (first row in a), starch (second row in a) and nonstructural carbohydrates (third row in a), and the ratio of soluble sugar to starch (b) across seasons and tissues.

Table 4. Comparisons of specific leaf area (*SLA*, $cm^2\ g^{-1}$), N (N_{mass}, %) and P (P_{mass}, $g\ kg^{-1}$) concentrations on a mass basis, cumulative water release of the stem (*CWR*, $g\ cm^{-3}$) and monthly growth rate of stem circumference (*CG*, μm) across seasons (in February, April and July).

	February	April	July
SLA	73.68 (2.25)b	116.14 (8.95)a	109.29 (6.05)a
N_{mass}	1.27 (0.08)b	1.56 (0.26)ab	1.59 (0.14)a
P_{mass}	0.56 (0.02)b	0.81 (0.05)a	0.94 (0.04)a
CWR	149.23 (24.08)b	357.66 (59.70)a	274.13 (27.04)a
CG for No. 3	−101	1720	504
CG for No. 4	3.1	23.2	4.5

Standard errors are shown in parentheses. Different letters indicate significant differences in leaf and stem traits across seasons.

SLA, N_{mass} and P_{mass}) and growth rate (low monthly change in stem circumference), coupled with *NSC* accumulation in February, may suggest a greater decline in growth relative to photosynthesis during the dry season in this plantation. In addition, lower stem water storage could be derived from the *CWR* and diurnal stem circumference pattern at lower soil water potential. The abovementioned conclusions support our second hypothesis that temporal dynamics of stomatal regulation behavior were accompanied by alterations in water- and carbon-related traits.

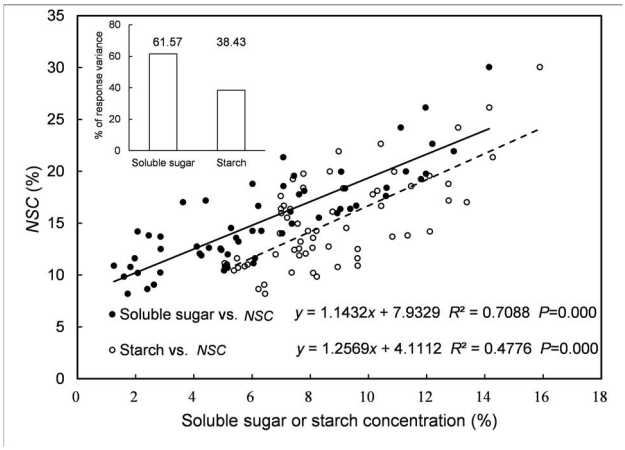

Figure 5. Correlation and contribution of soluble sugar and starch concentration to nonstructural carbohydrates (*NSC*) across seasons and tissues. The inset shows the relative importance of soluble sugar and starch concentrations for changes in *NSC*.

Stomatal regulation behavior in this *S. superba* plantation

Here, we demonstrated the stomatal regulation behavior of *S. superba* by analyzing the seasonal dynamics of $\psi_{\text{L-mid}}$ and stomatal responses to *VPD* using field measurements (Oren et al. 1999, Roman et al. 2015, Yi et al. 2017). In February, the $dG_s/dln(VPD)/G_{sref}$ of *S. superba* exhibited a relatively high value of 0.81, which may indicate strict stomatal regulation at lower soil water potentials. Similarly, Ogle et al. (2012) defined isohydric behavior using a normalized sensitivity ($dG_s/dln(VPD)/G_{sref}$) > 0.6. In addition, Roman et al. (2015) and Yi et al. (2017) suggested that isohydric species would exhibit a decrease in both G_s and $dG_s/dln(VPD)$ during drought periods. Consistent with their findings, the reduction in both G_{sref} and $dG_s/dln(VPD)$ in February may indicate that this *S. superba* plantation exhibited isohydric behavior during the dry season. More importantly, the constant $\psi_{\text{L-mid}}$ across different soil water potentials aligned with the original description of isohydric classification (Sperry et al. 2002). The isohydric strategy adopted in the dry season was also consistent with the results found by Jiang et al. (2021) for a small hydroscape area (0.87 MPa^2) calculated based on trajectories of $\psi_{\text{L-mid}}$ versus $\psi_{\text{L-pre}}$ in *S. superba*. The less strict stomatal regulation of desert species with increasing *VPD* (low $dG_s/ln(VPD)/G_{sref}$, 0.4 for desert species vs. 0.6 for a wide range of relatively mesic species) was due to the wider range of *VPD* (Oren et al. 1999), similar to the stomatal behavior in April and July in our study. Meanwhile, the significant difference in $\psi_{\text{L-mid}}$ between April and July also revealed the anisohydric behavior of *S. superba* during the wet season.

This *S. superba* plantation demonstrated isohydric behavior when subjected to a lower soil water potential, yet displayed anisohydric behavior under conditions of sufficient soil water status. This finding supported the conclusions of Hochberg et al. (2018) and Wu et al. (2021) that environmental conditions affected iso/anisohydry classifications. Changes in stomatal regulation behavior with growing environments may result from differences in maximum transpiration (Tramontini et al. 2014, Hochberg et al. 2018). A decrease in maximum transpiration could moderate the reduction in daily minimum ψ_L (Hochberg et al. 2018), which may have supported our results of isohydric behavior and lower F_d' in February. In addition, the anisohydric behavior under high soil water conditions could be associated with a high nighttime sap flux (Rogiers et al. 2009, Zhang et al. 2012). In this study, the mean nighttime sap flux densities (during 18:10–23:50 h) in February, April and July were 1.18 g m^{-2} s^{-1}, 4.48 g m^{-2} s^{-1} and 3.70 g m^{-2} s^{-1}, respectively, which may be one of the causes for the anisohydric behavior in April and July.

Seasonal variations in water- and carbon-related traits accompanied by stomatal regulation behaviors

In the present study, *S. superba* with strict stomatal control showed decreased water storage capacity (cumulative stem water release) and carbon gain (leaf economic traits, *SLA*, N_{mass} and P_{mass}) along with growth in February, whereas it showed increased *NSC* and constant stem hydraulic conductivity compared with those under higher soil water potentials. The results confirmed the conclusion of Carminati and Javaux (2020) that plants use stomatal strategies to maintain a minimal embolism risk and constant xylem conductance in response to environmental stress. The new xylem production, embolism repair and ionic effects have been acknowledged as crucial factors in maintaining hydraulic conductance under environmental stress conditions (Trifilò et al. 2014). Within this context, the importance of xylem anatomy and stem starch has gained significant attention (Eilmann et al. 2009, Salleo et al. 2009, Secchi et al. 2011). For instance, the coordination of vessel density and size was essential to maintain consistent xylem-specific hydraulic conductivity across a wide range of climatic conditions, demonstrating a homeostatic capacity of the xylem (Borghetti et al. 2016, García-Cervigón et al. 2020). Although this study observed a higher starch concentration in the dry season than the wet season, it is inconclusive to ascertain the impact of starch on embolism repair because xylem anatomy measurements were not taken. We instead hypothesized that the decreased water potential gradient, a result of strict stomatal regulation in the dry season, could induce a consistent xylem hydraulic conductivity under conditions of reduced sap flux density in this study. According to the growth-optimizing stomata model proposed by Potkay and Feng (2023), stomatal closure prevents water potential decrease, turgor loss and subsequent growth reduction on the one hand, and suppresses *NSC* through decreased photosynthetic carbon assimilation on the other hand. The temporal patterns of the water- and carbon-related traits in our study corroborated the decrease in carbon assimilation accompanied by strict stomatal behavior, while the growth-optimizing stomata model failed to explain the changes in *NSC* and growth. The observed reduction in radial stem growth during the dry season did not align with the results reported by Yan et al. (2012) in subtropical regions of China. Although *S. superba* grows throughout the year, Yan et al. (2012) found that the increase in *DBH* of *S. superba* measured using a dendrometer band was greater during the dry season than the wet season from April 2003 to March 2004 in the Dinghushan Biosphere Reserve, ~95 km from our study site. In Yan et al. (2012), *S. superba* was in the old-growth stage (> 400 years). However, the radial growth responses of trees of different ages to climate were different (Vieira et al. 2009), which may have caused the inconsistency between our results

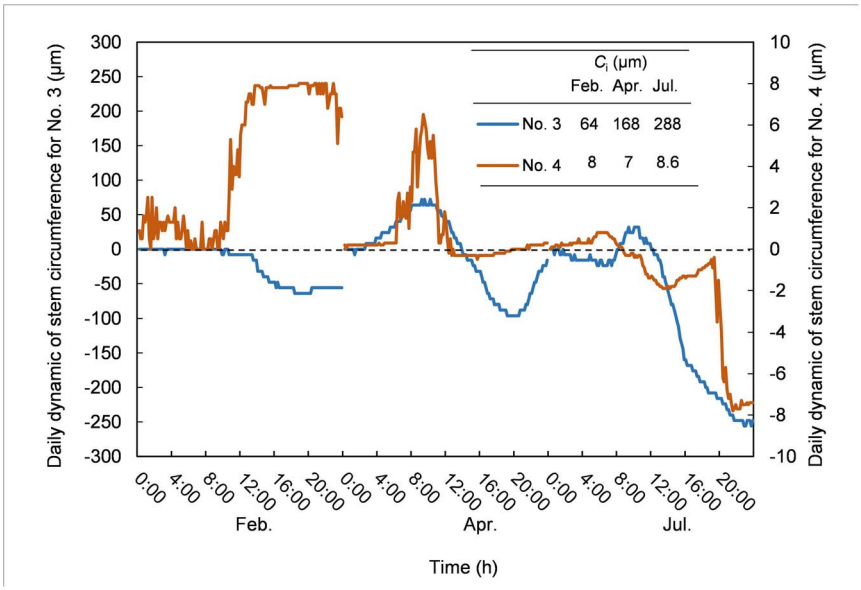

Figure 6. Daily dynamics and change range (C_i) of stem circumference for two sample trees on 15 February, 7 April and 10 July 2022. The stem circumference at 0:00 h on that day was used as the reference circumference. Data greater and less than 0 μm indicated trunk swelling and shrinkage, respectively. The daily range of change (C_i) in stem circumference in each month is inserted in the figure.

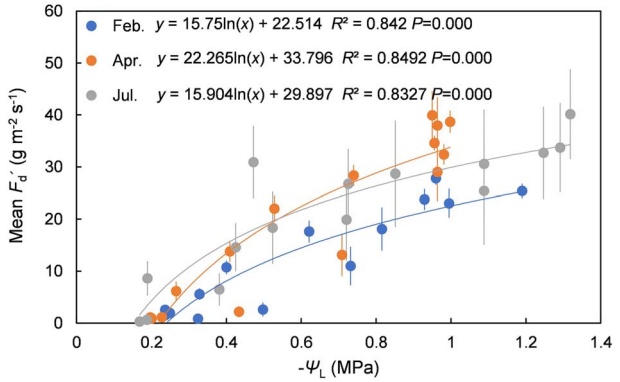

Figure 7. Relationship between mean sap flux density per unit sapwood area (F_d') and leaf water potential (Ψ_L) for four sample trees across months, on 15 February, 7 April and 10 July 2022. The regression equations are shown in the figure.

and those of Yan et al. (2012). In subtropical China, Huang et al. (2018) found a low rate of xylem formation for a coniferous species from early February to summer. The results of Huang et al. (2018) partially confirmed our result that radial growth was reduced in February. Although the increase in *NSC* and decrease in stem growth at lower soil water potential contradicted previous findings showing that trees typically deplete *NSC* during drought to prioritize growth (Doughty et al. 2015, Jones et al. 2020), our results were consistent with the growth limitation hypothesis that trees are not carbon deficient under current atmospheric conditions (Körner 2003). Würth et al. (2005) attributed the increase in *NSC* during dry seasons to drought-constrained growth. Similarly, in this study, accumulation of *NSC* in leaves could indicate a reduction in carbon requirements for growth (Palacio et al. 2018, Guo et al. 2022). The abovementioned conclusion may be due to the fact that growth is limited by environment conditions rather than carbon uptake, which leads to a carbon surplus under drought stress (Körner 2003, Würth et al. 2005, Franks et al. 2013). In addition, the lower *NSC* in *S. superba* observed in March than in January in subtropical China was attributed to the consumption of *NSC* reserves during leaf renewal in February (Chen et al. 2017), highlighting the effect of phenology on the temporal dynamics of *NSC*. However, the influence of phenology cannot be distinguished from the effects of environmental conditions on ecophysiological traits in this study. Therefore, future studies should be conducted during the same growing season with different climatic conditions to explicitly assess the ecophysiological responses of trees to environmental stresses.

In the present study, the increase in *SS* and *SS*/starch at lower soil water potential could play an important role in mediating water deficit responses. The enhancement of *SS* can be utilized for osmotic balance, facilitating the conversion of starch to *SS* and augmenting stress tolerance under unfavorable conditions (Kozlowski and Pallardy 2002, Chave et al. 2003, Bartels and Sunkar 2005, Ruelland et al. 2009, McDowell and Sevanto 2010, Gruber et al. 2011, Kannenberg and Phillips 2020). Similarly, a greater ratio of *SS* to *NSC* was observed in the dry season across an extensive precipitation gradient in Amazon forests (Signori-Müller et al. 2021). The elevated *SS* and reduced starch concentration in leaves in February may underscore the pivotal role of sugars in leaf functioning, including their ability to buffer against turgor loss and sustain assimilation (Gersony et al. 2020, Yang et al. 2022). Moreover, high levels of *NSC* in the xylem facilitate the repair of embolisms and provide osmoprotection against stress (Plavcová and Jansen 2015). In line with the finding that branches act as the major buffer for seasonal variation in carbon demand (Newell et al. 2002), the relatively high seasonal variability of *NSC* and their two components in branches and phloem in this study indicated that branches and phloem played an important role in maintaining the carbon cycle in trees. Therefore, the accumulation of *NSC* may assist in maintaining a stable water potential within the species, which is coordinated with isohydric stomatal behavior at lower soil water potential.

In this study, the cumulative water release of *S. superba* decreased with decreasing soil water potential, which was accompanied by stomatal isohydric behavior. Similarly, it has been reported that the stem water storage of *Quercus ilex* L. is depleted during the dry season in a Mediterranean forest (Zweifel et al. 2000, Lempereur et al. 2015). Yi et al. (2017) showed that isohydric sugar maples were less reliant on water stored in the stem than anisohydric species. However, the contributions of high stem hydraulic conductivity and water storage to a stable $\Psi_{L\text{-}mid}$ have been reported (Scholz et al. 2007, Gleason et al. 2012, Matheny et al. 2015, Simonin et al. 2015, Fu et al. 2019). The limited water storage capacity in the stems of anisohydric species may be attributed to their dense wood and enhanced embolism resistance at the interspecies level (Hoffmann et al. 2011, Martínez-Vilalta et al. 2014, Simonin et al. 2015, Fu et al. 2019, Fu and Meinzer 2019). The aforementioned conclusions do not appear to hold for our intraspecific study, where anisohydric behavior, a higher reference F_d' and relatively large stem water storage of *S. superba* were observed under conditions of sufficient water availability. This could be due to a closer association between water storage and hydraulic traits, such as vessel size (Kocher et al. 2013, Plavcová and Jansen 2015, Pratt and Jacobsen 2017, Janssen et al. 2020), rather than stomatal control. For example, high water storage was associated with high vessel fraction and efficient water transport and vice versa (Limousin et al. 2010, Gleason et al. 2012, Fu et al. 2019), which is supported by our results showing higher reference F_d' and relatively large stem water storage in April and July. Thus, the measurement of anatomical structures in xylem across seasons could potentially provide substantial evidence for the hydraulic properties of stomatal regulation within species in future studies.

In our study, the temporal patterns of water storage and *NSC* may have shown a trade-off between water and carbon storage suggested by Jiang et al. (2021). Because *NSC* accumulation can be used to maintain osmotic regulation and water potential in trees, which contributes to drought tolerance (Adams et al. 2013, Mitchell et al. 2013, Dickman et al. 2015), stored water, which may relieve the increasing tension in the xylem sap, may not be fully required during water stress. In addition, both water and *NSC* are stored in xylem, and the limited fraction of xylem volume can cause a trade-off between water storage and *NSC* (Ziemińska et al. 2013, Plavcová et al. 2016, Thalmann and Santelia 2017, von Arx et al. 2017). Jiang et al. (2021) elucidated the trade-off between xylem water and carbohydrate storage in the stem of subtropical pine plantations, and our study may provide new evidence for such an association within species across seasons.

Conclusions

The objective of this research was to investigate the temporal dynamics of water- and carbon-related traits and stomatal regulation behavior for native tree species in low subtropical China. We confirmed that stomatal regulation behavior is dependent on soil water status, and identified an isohydric strategy for *S. superba* at lower soil water potentials and anisohydric behavior at higher soil water potentials. Soluble sugar contributed more to the temporal dynamics of *NSC* than starch. The low growth rate and starch accumulation may indicate a carbon sink limitation. Because of the increased *NSC* and decreased water storage under lower soil water potentials, a trade-off between carbon and water storage can be speculated. Therefore, our results provide insights into plant carbon and water process models under changing climate scenarios. However, this study has several limitations. For example, as an important carbohydrate sink tissue, root system is critical for *NSC* storage and water uptake (Matheny et al. 2015, Martínez-Vilalta et al. 2016, Plavcová et al. 2016, Li et al. 2018), which was not involved in our study. Therefore, the temporal dynamics of *NSC* in roots should be considered in future studies of water and carbon processes in forests.

Supplementary data

Supplementary data for this article are available at *Tree Physiology* Online.

Funding

This work was funded by the National Nature Science Foundation of China (32171501, 31770646 to L.-W.Z.) and the Basic and Applied Basic Research Foundation of Guangdong Province (2021A1515012486 to L.-W.Z.).

Authors' contributions

L.-W.Z. designed the study, performed data analyses and wrote the draft. Y.-Q.L., L.-W.L., J.-Y.W. and J.D. conducted the experiment, and P.Z. revised the manuscript.

Data availability statement

The data that support the findings of this study and code in analysis are available from the first author, L.-W.Z., upon reasonable request.

References

Adams HD, Guardiola-Claramonte M, Barron-Gafford GA, Villegas JC, Breshears DD, Zou CB, Troch PA, Huxman TE (2009) Temperature sensitivity of drought-induced tree mortality portends increased regional die-off under global-change-type drought. Proc Natl Acad Sci USA 106:7063–7066.

Adams HD, Germino MJ, Breshears DD, Barron-Gafford GA, Guardiola-Claramonte M, Zou CB, Huxman TE (2013) Nonstructural leaf carbohydrate dynamics of *Pinus edulis* during drought-induced tree mortality reveal role for carbon metabolism in mortality mechanism. New Phytol 197:1142–1151.

Anderegg WRL, Kane JM, Anderegg LDL (2013) Consequences of widespread tree mortality triggered by drought and temperature stress. Nat Clim Chang 3:30–36.

Bartels D, Sunkar R (2005) Drought and salt tolerance in plants. Crit Rev Plant Sci 24:23–58.

Borghetti M, Gentilesca T, Leonardi S, van Noije T, Rita A (2016) Long-term temporal relationships between environmental conditions and xylem functional traits: a meta-analysis across a range of woody species along climatic and nitrogen deposition gradients. Tree Physiol 37:4–17.

Brodribb TJ, Cochard H (2009) Hydraulic failure defines the recovery and point of death in water-stressed conifers. Plant Physiol 149: 575–584.

Bucci SJ, Goldstein G, Meinzer FC, Franco AC, Campanello P, Scholz FG (2005) Mechanisms contributing to seasonal homeostasis of minimum leaf water potential and predawn disequilibrium between soil and plant water potential in Neotropical savanna trees. Trees 19:296–304.

Campbell GS, Norman JM (1998). An introduction to environmental biophysics (2nd edn). Springer Science + Business Media, Inc., New York, NY. https://doi.org/10.1007/978-1-4612-1626-1.

Carminati A, Javaux M (2020) Soil rather than xylem vulnerability controls stomatal response to drought. Trends Plant Sci 25:868–880.
Chave MM, Maroco JP, Pereira JS (2003) Understanding plant responses to drought-from genes to the whole plant. Funct Plant Biol 30:239–264.
Chen ZC, Wang L, Dai YX, Wan XC, Liu SR (2017) Phenology-dependent variation in the non-structural carbohydrates of broadleaf evergreen species plays an important role in determining tolerance to defoliation (or herbivory). Sci Rep 7:10125. https://doi.org/10.1038/s41598-017-09757-2.
Choat B, Jansen S, Brodribb TJ et al. (2012) Global convergence in the vulnerability of forests to drought. Nature 491:752–755.
Collins MJ, Fuentes S, Barlow EWR (2010) Partial rootzone drying and deficit irrigation increase stomatal sensitivity to vapour pressure deficit in anisohydric grapevines. Funct Plant Biol 37:128–138.
Dickman LT, McDowell NG, Sevanto S, Pangle RE, Pockman WT (2015) Carbohydrate dynamics and mortality in a piñon-juniper woodland under three future precipitation scenarios. Plant Cell Environ 38:729–739.
Dietze MC, Sala A, Carbone MS, Czimczik CI, Mantooth JA, Richardson AD, Vargas R (2014) Nonstructural carbon in woody plants. Annu Rev Plant Biol 65:667–687.
Domec JC, Johnson DM (2012) Does homeostasis or disturbance of homeostasis in minimum leaf water potential explain the isohydric versus anisohydric behavior of *Vitis vinifera* L. cultivars? Tree Physiol 32:245–248.
Doughty CE, Metcalfe DB, Girardin CAJ et al. (2015) Source and sink carbon dynamics and carbon allocation in the Amazon basin. Global Biogeochem Cycles 29:645–655.
Eilmann B, Zweifel R, Buchmann N, Fonti P, Rigling A (2009) Drought induced adaptation of xylem in Scots pine and pubescent oak. Tree Physiol 29:1011–1020.
Franks PJ, Adams MA, Amthor JS et al. (2013) Sensitivity of plants to changing atmospheric CO_2 concentration: from geological past to the next century. New Phytol 197:1077–1094.
Fu XL, Meinzer FC (2019) Metrics and proxies for stringency of regulation of plant water status (iso/anisohydry): a global data set reveals coordination and trade-offs among water transport traits. Tree Physiol 39:122–134.
Fu XL, Meinzer FC, Woodruff DR, Liu Y-Y, Smith DD, McCulloh KA, Howard AR (2019) Coordination and trade-offs between leaf and stem hydraulic traits and stomatal regulation along a spectrum of isohydry to anisohydry. Plant Cell Environ 42:2245–2258.
García-Cervigón AI, Fajardo A, Caetano-Sánchez C, Julio Camarero J, Miguel Olano J (2020) Xylem anatomy needs to change, so that conductivity can stay the same: xylem adjustments across elevation and latitude in *Nothofagus pumilio*. Ann Bot 125:1101–1112.
Garcia-Forner N, Biel C, Savé R, Martínez-Vilalta J (2017) Isohydric species are not necessarily more carbon limited than anisohydric species during drought. Tree Physiol 37:441–455.
Gersony JT, Hochberg U, Rockwell FE, Park M, Gauthier PPG, Holbrook NM (2020) Leaf carbon export and nonstructural carbohydrates in relation to diurnal water dynamics in mature oak trees. Plant Physiol 183:1612–1621.
Gleason SM, Butler DW, Zieminska K, Waryszak P, Westoby M (2012) Stem xylem conductivity is key to plant water balance across Australian angiosperm species. Funct Ecol 26:343–352.
Granier A (1987) Evaluation of transpiration in a Douglas fir stands by means of sapflow measurements. Tree Physiol 3:309–320.
Grömping U (2007) Estimators of relative importance in linear regression based on variance decomposition. Am Stat 61:139–147.
Gruber A, Pirkebner D, Florian C, Oberhuber W (2011) No evidence for depletion of carbohydrate pools in Scots pine (*Pinus sylvestris* L.) under drought stress. Plant Biol 14:142–148.
Guo XW, Liu SR, Wang H et al. (2022) Divergent allocations of non-structural carbohydrates shape growth response to rainfall reduction in two subtropical plantations. For Ecosyst 9:100021. https://doi.org/10.1016/j.fecs.2022.100021.
Hartmann H, Moura CF, Anderegg WRL et al. (2018) Research frontiers for improving our understanding of drought-induced tree and forest mortality. New Phytol 218:15–28.
Hochberg U, Rockwell FE, Holbrook NM, Cochard H (2018) Iso/anisohydry: a plant-environment interaction rather than a simple hydraulic trait. Trends Plant Sci 23:112–120.
Hoffmann WA, Marchin RM, Abit P, Lau OL (2011) Hydraulic failure and tree dieback are associated with high wood density in a temperate forest under extreme drought. Glob Chang Biol 17:2731–2742.
Hölttä T, Mencuccini M, Nikinmaa E (2009) Linking phloem function to structure: analysis with a coupled xylem-phloem transport model. J Theor Biol 259:325–337.
Huang JG, Guo XL, Rossi S, Zhai LH, Yu BY, Zhang SK, Zhang MF (2018) Intra-annual wood formation of subtropical Chinese red pine shows better growth in dry season than wet season. Tree Physiol 38: 1225–1236.
Janssen TAJ, Hölttä T, Fleischer K, Naudts K, Dolman H (2020) Wood allocation trade-offs between fiber wall, fiber lumen and axial parenchyma drive drought resistance in neotropical trees. Plant Cell Environ 43:965–980.
Jiang PP, Meinzer FC, Fu XL, Kou L, Dai XQ, Wang HM (2021) Trade-offs between xylem water and carbohydrate storage among 24 coexisting subtropical understory shrub species spanning a spectrum of isohydry. Tree Physiol 41:403–415.
Jones S, Rowland L, Cox P et al. (2020) The impact of a simple representation of non-structural carbohydrates on the simulated response of tropical forests to drought. Biogeosciences 17:3589–3612.
Kannenberg SA, Phillips RP (2020) Non-structural carbohydrate pools not linked to hydraulic strategies or carbon supply in tree saplings during severe drought and subsequent recovery. Tree Physiol 40: 259–271.
Kaplick J, Clearwater MJ, Macinnis-Ng C (2018) Stem water storage of New Zealand kauri (*Agathis australis*). Acta Hortic 1222:59–66.
Klein T (2014) The variability of stomatal sensitivity to leaf water potential across species indicates a continuum between isohydric and anisohydric behaviours. Funct Ecol 28:1313–1320.
Kocher P, Horna V, Leuschner C (2013) Stem water storage in five coexisting temperate broad-leaved tree species: significance, temporal dynamics and dependence on tree functional traits. Tree Physiol 33:817–832.
Körner C (2003) Carbon limitation in trees. J Ecol 91:4–17.
Kozlowski TT, Pallardy S (2002) Acclimation and adaptive responses of woody plants to environmental stresses. Bot Rev 68:270–334.
Kumagai T, Aoki S, Otsuki K, Utsumi Y (2009) Impact of stem water storage on diurnal estimations of whole-tree transpiration and canopy conductance from sap flow measurements in Japanese cedar and Japanese cypress trees. Hydrol Process 23:2335–2344.
Lambers H, Poorter H (1992) Inherent variation in growth rate between higher plants: a search for physiological causes and ecological consequences. Adv Ecol Res 23:187–261.
Lempereur M, Martin-StPaul NK, Damesin C, Joffre R, Ourcival JM, Rocheteau A, Rambal S (2015) Growth duration is a better predictor of stem increment than carbon supply in a Mediterranean oak forest: implications for assessing forest productivity under climate change. New Phytol 207:579–590.
Li WB, Hartmann H, Adams HD et al. (2018) The sweet side of global change-dynamic responses of non-structural carbohydrates to drought, elevated CO_2 and nitrogen fertilization in tree species. Tree Physiol 38:1706–1723.
Li WB, McDowell NG, Zhang HX, et al. (2022) The influence of increasing atmospheric CO_2, temperature, and vapor pressure deficit on seawater-induced tree mortality. New Phytol 235: 1767–1779.
Limousin JM, Longepierre D, Huc R, Rambal S (2010) Change in hydraulic traits of Mediterranean *Quercus ilex* subjected to long-term throughfall exclusion. Tree Physiol 30:1026–1036.
Liu YL, Parolari AJ, Kumar M, Huang C-W, Katul GG, Porporato A (2017) Increasing atmospheric humidity and CO_2

concentration alleviate forest mortality risk. Proc Natl Acad Sci USA 114:9918–9923.
Liu ZQ, Liu QQ, Wei ZJ, Yu XX, Jia GD, Jiang J (2021) Partitioning tree water usage into storage and transpiration in a mixed forest. For Ecosyst 8:72. https://doi.org/10.1186/s40663-021-00353-5.
Martínez-Vilalta J, Garcia-Forner N (2017) Water potential regulation, stomatal behaviour and hydraulic transport under drought: deconstructing the iso/anisohydric concept. Plant Cell Environ 40: 962–976.
Martínez-Vilalta J, Poyatos R, Aguadé D, Retana J, Mencuccini M (2014) A new look at water transport regulation in plants. New Phytol 204:105–115.
Martínez-Vilalta J, Sala A, Asensio D, Galiano L, Hoch G, Palacio S, Piper FI, Lloret F (2016) Dynamics of non-structural carbohydrates in terrestrial plants: a global synthesis. Ecological monographs 86: 495–516.
Matheny AM, Bohrer G, Garrity SR, Morin TH, Howard CJ, Vogel CS (2015) Observations of stem water storage in trees of opposing hydraulic strategies. Ecosphere 6:1–13.
McDowell NG, Sevanto S (2010) The mechanisms of carbon starvation: how, when, or does it even occur at all? New Phytol 186:264–266.
McDowell N, Pockman WT, Allen CD et al. (2008) Mechanisms of plant survival and mortality during drought: why do some plants survive while others succumb to drought? New Phytol 178: 719–739.
Meinzer FC, Woodruff AL, Marias DE, Smith DD, McCulloh KA, Howard AR, Magedman AL (2016) Mapping 'hydroscapes' along the iso- to anisohydric continuum of stomatal regulation of plant water status. Ecol Lett 19:1343–1352.
Meinzer FC, Smith DD, Woodruff DR, Marias DE, McCulloh KA, Howard AR, Magedman AL (2017) Stomatal kinetics and photosynthetic gas exchange along a continuum of isohydric to anisohydric regulation of plant water status. Plant Cell Environ 40: 1618–1628.
Mitchell PJ, Ogrady AP, Tissue DT, White DA, Ottenschlaeger ML, Pinkard EA (2013) Drought response strategies define the relative contributions of hydraulic dysfunction and carbohydrate depletion during tree mortality. New Phytol 197:862–872.
Newell EA, Mulkey SS, Wright SJ (2002) Seasonal patterns of carbohydrate storage in four tropical tree species. Oecologia 131:333–342.
Novick KA, Ficklin DL, Baldocchi D et al. (2022) Confronting the water potential information gap. Nat Geosci 15:158–164.
Ogle K, Lucas RW, Bentley LP et al. (2012) Differential daytime and night-time stomatal behavior in plants from North American deserts. New Phytol 194:464–476.
Oren R, Sperry JS, Katul GG, Pataki DE, Ewers BE, Phillips N, Schäfer KVR (1999) Survey and synthesis of intra- and interspecific variation in stomatal sensitivity to vapour pressure deficit. Plant Cell Environ 22:1515–1526.
Ouyang L, Lu LW, Wang CL et al. (2022) A 14-year experiment emphasizes the important role of heat factors in regulating tree transpiration, growth, and water use efficiency of *Schima superba* in South China. Agric Water Manag 273:107902. https://doi.org/10.1016/j.agwat.2022.107902.
Palacio S, Camarero JJ, Maestro M, Alla AQ, Lahoz E, Montserrat–Martí G (2018) Are storage and tree growth related? Seasonal nutrient and carbohydrate dynamics in evergreen and deciduous Mediterranean oaks. Trees 32:777–790.
Plaut JA, Yepez EA, Hill J, Pangle R, Sperry JS, Pockman WT, McDowell NG (2012) Hydraulic limits preceding mortality in a piñon-juniper woodland under experimental drought. Plant Cell Environ 35: 1601–1617.
Plavcová L, Jansen S (2015). The role of xylem parenchyma in the storage and utilization of nonstructural carbohydrates. In: Hacke U (ed.) Functional and ecological xylem anatomy. Springer International Publishing, Cham, Switzerland, pp 209–234.
Plavcová L, Hoch G, Morris H, Ghiasi S, Jansen S (2016) The amount of parenchyma and living fibers affects storage of nonstructural carbohydrates in young stems and roots of temperate trees. Am J Bot 103:603–612.
Poni S, Bernizzoni F, Civardi S (2007) Response of 'Sangiovese' grapevines to partial root-zone drying: gas-exchange, growth and grape composition. Sci Hortic 114:96–103.
Potkay A, Feng X (2023) Do stomata optimize turgor-driven growth? A new framework for integrating stomata response with whole-plant hydraulics and carbon balance. New Phytol 238:506–528.
Pratt RB, Jacobsen AL (2017) Conflicting demands on angiosperm xylem: tradeoffs among storage, transport and biomechanics. Plant Cell Environ 40:897–913.
Rogiers SY, Greer DH, Hutton RJ, Landsberg JJ (2009) Does night-time transpiration contribute to anisohydric behaviour in a *Vitis vinifera* cultivar? J Exp Bot 60:3751–3763.
Roman DT, Novick KA, Brzostek ER, Dragoni D, Rahman F, Phillips RP (2015) The role of isohydric and anisohydric species in determining ecosystem-scale response to severe drought. Oecologia 179: 641–654.
Rosas T, Mencuccini M, Barba J, Cochard H, Saura-Mas S, Martínez-Vilalta J (2019) Adjustments and coordination of hydraulic, leaf and stem traits along a water availability gradient. New Phytol 223:632–646.
Ruehr NK, Offermann CA, Gessler A, Winkler JB, Ferrio JP, Buchmann N, Barnard RL (2009) Drought effects on allocation of recent carbon: from beech leaves to soil CO_2 efflux. New Phytol 184: 950–961.
Ruelland E, Vaultier MN, Zachowski A, Hurry V (2009) Cold signalling and cold acclimation in plants. In: Kader JC, Delseny M (eds) Advances in botanical research. Academic Press, San Diego, CA, pp 35–150.
Salleo S, Trifilò P, Esposito S, Nardini A, Lo Gullo MA (2009) Starch-to-sugar conversion in wood parenchyma of field-growing *Laurus nobilis* plants: a component of the signal pathway for embolism repair? Funct Plant Biol 36:815–825.
Schäfer KAR, Oren R, Tenhunen JD (2000) The effect of tree height on crown level stomatal conductance. Plant Cell Environ 23:365–375.
Scholz FG, Buccie SJ, Goldstein G, Meinzer FC, Franco AC, Miralles-Wilhelm F (2007) Biophysical properties and functional significance of stem water storage tissues in Neotropical savanna trees. Plant Cell Environ 30:236–248.
Scholz FG, Phillips NG, Bucci SJ, Meinzer FC, Goldstein G (2011) Hydraulic capacitance: biophysics and functional significance of internal water sources in relation to tree size. Springer, Dordrecht, The Netherlands. https://doi.org/10.1007/978-94-007-1242-3_13.
Secchi F, Gilbert ME, Zwieniecki MA (2011) Transcriptome response to embolism formation in stems of *Populus trichocarpa* provides insight into signalling and the biology of refilling. Plant Physiol 157: 1419–1429.
Signori-Müller C, Oliveira RS, Barros FdV, et al. (2021) Non-structural carbohydrates mediate seasonal water stress across Amazon forests. Nat Commun 12:1–9.
Simonin KA, Burns E, Choat B, Barbour MM, Dawson TE, Franks PJ (2015) Increasing leaf hydraulic conductance with transpiration rate minimizes the water potential drawdown from stem to leaf. J Exp Bot 66:1303–1315. https://doi.org/10.1093/jxb/eru481.
Sperry JS, Hacke UG, Oren R, Comstock JP (2002) Water deficits and hydraulic limits to leaf water supply. Plant Cell Environ 25:251–263.
Steppe K, Sterck F, Deslauriers A (2015) Diel growth dynamics in tree stems: linking anatomy and ecophysiology. Trends Plant Sci 20: 335–343.
Tardieu F, Simonneau T (1998) Variability among species of stomatal control under fluctuating soil water status and evaporative demand: modelling isohydric and anisohydric behaviours. J Exp Bot 49: 419–432.
Thalmann M, Santelia D (2017) Starch as a determinant of plant fitness under abiotic stress. New Phytol 214:943–951.
Tomasella M, Casolo V, Aichner N, Petruzzellis F, Savi T, Trifilò P, Nardini A (2019) Non-structural carbohydrate and hydraulic

dynamics during drought and recovery in *Fraxinus ornus* and *Ostrya carpinifolia* saplings. Plant Physiol Biochem 145:1–9.
Tramontini S, Döring J, Vitali M, Ferrandino A, Stoll M, Lovisolo C (2014) Soil water-holding capacity mediates hydraulic and hormonal signals of near-isohydric and near-anisohydric *Vitis* cultivars in potted grapevines. Funct Plant Biol 41:1119–1128.
Trifilò P, Barbera PM, Raimondo F, Nardini A, Lo Gullo MA (2014) Coping with drought-induced xylem cavitation: coordination of embolism repair and ionic effects in three Mediterranean evergreens. Tree Physiol 34:109–122.
Trifilò P, Kiorapostolou N, Petruzzellis F, Vitti S, Petit G, Lo Gullo MA, Nardini A, Casolo V (2019) Hydraulic recovery from xylem embolism in excised branches of twelve woody species: relationships with parenchyma cells and non-structural carbohydrates. Plant Physiol Biochem 139:513–520.
von Arx G, Zrzac A, Fonti P, Frank D, Zweifel R, Rigling A, Galiano L, Gesseler A, Olano JM (2017) Responses of sapwood ray parenchyma and non-structural carbohydrates of *Pinus sylvestris* to drought and long-term irrigation. Funct Ecol 31: 1371–1382.
Vieira J, Campelo F, Nabais C (2009) Age-dependent responses of tree-ring growth and intra-annual density fluctuations of *Pinus pinaster* to Mediterranean climate. Trees 23:257–265.
Woodruff DR, Meinzer FC (2011) Water stress, shoot growth and storage of non-structural carbohydrates along a tree height gradient in a tall conifer. Plant Cell Environ 34:1920–1930.
Woodruff DR, Meinzer FC, Marias DE, Sevanto S, Jenkins MW, McDowell NG (2015) Linking nonstructural carbohydrate dynamics to gas exchange and leaf hydraulic behavior in *Pinus edulis* and *Juniperus monosperma*. New Phytol 206:411–421.
Wright IJ, Reich PB, Westoby M et al. (2004) The worldwide leaf economics spectrum. Nature 428:821–827.
Wu GH, Guan KY, Li Y et al. (2021) Interannual variability of ecosystem iso/anisohydry is regulated by environmental dryness. New Phytol 229:2562–2575.
Würth MKR, Peláez-Riedl S, Wright SJ, Körner C (2005) Non-structural carbohydrate pools in a tropical forest. Oecologia 143: 11–24.
Xu G-Q, Chen T-Q, Liu S-S, Ma J, Li Y (2023) Within-crown plasticity of hydraulic properties influence branch dieback patterns of two woody plants under experimental drought conditions. Sci Total Environ 854:158802. https://doi.org/10.1016/j.scitotenv.2022.158802.
Yan JH, Liu XZ, Tang XL, Yu GR, Zhang LM, Chen QQ, Li K (2012) Substantial amounts of carbon are sequestered during dry periods in an old-growth subtropical forest in South China. J For Res 18: 21–30.
Yang XJ, Jiang Y, Xue F, Ding XY, Cui MH, Dong MY, Kang MY (2022) Soil moisture controls on the dynamics of nonstructural carbohydrate storage in *Picea meyeri* during the growing season. Agric For Meteorol 326:109162. https://doi.org/10.1016/j.agrformet.2022.109162.
Yi K, Dragoni D, Phillips RP, Roman DT, Novick KA (2017) Dynamics of stem water uptake among isohydric and anisohydric species experiencing a severe drought. Tree Physiol 37:1379–1392.
Zhang YQ, Oren R, Kang SZ (2012) Spatiotemporal variation of crown-scale stomatal conductance in an arid *Vitis vinifera* L. cv. Merlot vineyard: direct effects of hydraulic properties and indirect effects of canopy leaf area. Tree Physiol 32:262–279.
Zhang ZZ, Zhao P, McCarthy HR, Zhao XH, Niu JF, Zhu LW, Ni GY, Ouyang L, Huang YQ (2016) Influence of the decoupling degree on the estimation of canopy stomatal conductance for two broadleaf tree species. Agric For Meteorol 221:230–241.
Zhu L-W, Zhao P (2023) Climate-driven sapwood-specific hydraulic conductivity and the Huber value but not leaf-specific hydraulic conductivity on a global scale. Sci Total Environ 857:159334. https://doi.org/10.1016/j.scitotenv.2022.159334.
Zhu S-D, Song J-J, Li R-H, Ye Q (2013) Plant hydraulics and photosynthesis of 34 woody species form different successional stages of subtropical forests. Plant Cell Environ 36:879–891.
Ziemińska K, Butler DW, Gleason SM, Wright IJ, Westoby M (2013) Fibre wall and lumen fractions drive wood density variation across 24 Australian angiosperms. AoB Plants 5:plt046. https://doi.org/10.1093/aobpla/plt046.
Zweifel R, Item H, Häsler R (2000) Stem radius changes and their relation to stored water in stems of young Norway spruce trees. Trees 15:50–57.

Tree Physiology, 2024, 44, 246–259
https://doi.org/10.1093/treephys/tpae016
Research paper